The Polar Region Consecutive to the HIV Fusion Peptide Participates in Membrane Fusion†

Sergio Gerardo Peisajovich,‡ Raquel F. Epand,§ Moshe Pritsker,‡ Yechiel Shai,‡ and Richard M. Epand*,§

Department of Biological Chemistry, Weizmann Institute of Science, Rehovot 76100, Israel, and Department of Biochemistry, McMaster University Health Sciences Centre, Hamilton, Ontario L8N 3Z5, Canada

Received August 12, 1999; Revised Manuscript Received December 7, 1999

ABSTRACT: The fusion peptide of HIV-1 gp41 is formed by the 16 N-terminal residues of the protein. This 16-amino acid peptide, in common with several other viral fusion peptides, caused a reduction in the bilayer to hexagonal phase transition temperature of dipalmitoleoylphosphatidylethanolamine (T_H), suggesting its ability to promote negative curvature in membranes. Surprisingly, an elongated peptide corresponding to the 33 N-terminal amino acids raised T_H, although it was more potent than the 16-amino acid fusion peptide in inducing lipid mixing with large unilamellar liposomes of 1:1:1 dioleoylphosphatidylethanolamine/dioleoylphosphatidylcholine/cholesterol. The 17-amino acid C-terminal fragment of the peptide can induce membrane fusion by itself, if it is anchored to a membrane by palmitoylation of the amino terminus, indicating that the additional 17 hydrophilic amino acids contribute to the fusogenic potency of the peptide. This is not solely a consequence of the palmitoylation, as a random peptide with the same amino acid composition with a palmitoyl anchor was less potent in promoting membrane fusion and palmitic acid itself had no fusogenic activity. The 16-amino acid N-terminal fusion peptide and the longer 33-amino acid peptide were labeled with NBD. Fluorescence binding studies indicate that both peptides bind to the membrane with similar affinities, indicating that the increased fusogenic activity of the longer peptide was not a consequence of a greater extent of membrane partitioning. We also determined the secondary structure of the peptides using FTIR spectroscopy. We find that the amino-terminal fusion peptide is inserted into the membrane as a β-sheet and the 17 C-terminal amino acids lie on the surface of the membrane, adopting an α-helical conformation. It was further demonstrated with the use of rhodamine-labeled peptides that the 33-amino acid peptide self-associated in the membrane while the 16-amino acid N-terminal peptide did not. Thus, the 16-amino acid N-terminal fusion peptide of HIV inserts into the membrane and, like other viral fusion peptides, lowers T_H. In addition, the 17 consecutive amino acids enhance the fusogenic activity of the fusion peptide presumably by promoting its self-association.

Elucidation of the mechanism of the fusion of enveloped viruses to target membranes has attracted considerable attention because of its relative simplicity and potential clinical importance. Apart from the functions of viral binding to target membranes and the activation of viral fusion proteins, usually only one viral protein is responsible for the actual membrane fusion step. The amino acid sequence and even the crystallographic structure of the ectodomain of several viral fusion proteins are known. This is also the case for fusion protein gp41 of HIV (*1*, *2*). However, the nature of the interaction of viral fusion proteins with membranes and the mechanism by which these proteins accelerate the formation of membrane fusion intermediates are poorly understood.

For several viruses, a small segment has been identified as the viral fusion peptide. The properties of viral fusion peptides are such that when this segment of the protein is made into a synthetic peptide, this peptide has certain membrane perturbing properties. In a few cases, including the HIV fusion peptide (*3*−*6*), the fusion peptide can also accelerate the rate of liposome fusion in model systems. It has been shown that the L- and D-enantiomorphs of the 33-amino acid N-terminal peptide of gp41 function equally well in promoting liposome fusion (*7*). This would suggest that a stereochemically specific interaction between the fusion peptide and the membrane is not required.

The fusion peptides of several viruses are found at the amino terminus of the processed fusion protein. In the case of HIV, mutation of this region in the intact viral fusion protein leads to a loss of fusogenic activity. It has been shown that the V2E mutant of the HIV fusion peptide is inactive in membrane fusion (*8*). Interestingly, this inactive mutant was shown to adopt predominantly α-helical structure (*9*). Even though this evidence could suggest a requirement for a β-structure, several viral fusion peptides have also been shown to adopt an α-helical conformation and to insert at an oblique angle into a bilayer (*10*−*12*), including the HIV (*5*, *12*) and the related SIV (*13*, *14*) fusion peptides. This mode of insertion has been associated with viral infectivity in the case of HIV (*14*, *15*). However, a characteristic of

† This work was supported by a grant from the Medical Research Council of Canada (MT-7654).

* Corresponding author. Phone: (905) 525-9140, ext. 22073. Fax: (905) 522-9033. E-mail: epand@fhs.csu.mcmaster.ca.

‡ Weizmann Institute of Science.

§ McMaster University Health Sciences Centre.

10.1021/bi991887i CCC: $19.00
Published on Web 01/29/2000

many fusion peptides is that they can readily interconvert between α-helical and β-structure conformations. It is possible that the conversion of an α-helical structure to the more extended β-conformation plays an important role during membrane fusion to allow access of the fusion peptide to the trans monolayer of the target membrane (*16*). A feature common to many viral fusion peptides is that they lower the bilayer to hexagonal phase transition temperature (T_H)[1] (*16*). However, the effects of these peptides on membrane curvature, as measured by hexagonal phase cylinder diameter, are small (*17*) and in some cases not experimentally measurable (*18*). There may also be other physical properties, such as length mismatch (*19*), the lowering of the membrane rupture tension (*20*), or the aggregation of the peptide (*21*, *22*), that facilitate formation of fusion pores.

Most studies of viral fusion peptides have used peptides of ≤20 amino acids. With many viruses, the length of the fusion peptide is thought to be in the range of 10−15 amino acids, and a polar amino acid often follows the amino-terminal fusion peptide. However, it has been shown in the case of the N-terminal, 20-amino acid influenza fusion peptide that addition of residues 21−127 to this peptide markedly increases its fusogenicity (*23*). The 127-amino acid peptide contained the coiled-coil region of the protein. The increased fusogenicity of this 127-amino acid construct may be caused by trimerization, allowing three fusion peptides to be present within a single protein aggregate. In the case of the HIV fusion protein gp41, there is a minimum length required for the peptide to increase the electrical conductivity of the bilayer (*24*). With the related SIV fusion peptides, a short 12-amino acid peptide is more effective than a longer 24-amino acid peptide (*12*). Thus, the relationship of peptide length to fusion potency is not simple. For the N-terminus of the HIV fusion protein, there is a clear change in hydrophobicity between the first 16 amino acids at the amino terminus and the following 17 amino acids. The sequence of the first 33 amino acids of this protein segment is AVGIGALFLGFLGAAGSTMGARSMTLTVQARQL. The sequence of the first 16 amino acids, containing the fusion peptide, contains no charged or polar amino acid residues. However, residues 17 and 18 are Ser and Thr, respectively, and the segment of residues 17−33 contains two positively charged amino acid residues and seven other polar amino acids. One would not anticipate that the segment of residues 17−33 readily inserts into membranes. Thus, if the lengthening of the 16-amino acid fusion peptide of HIV results in an increased rate of membrane fusion, it would not be a consequence of the direct insertion of the carboxyl-terminal segment into membranes.

[1] Abbreviations: ANTS, 8-aminonaphthalene-1,3,6-trisulfonic acid; ATR-FTIR, attenuated total reflection Fourier-transformed infrared spectroscopy; BOC, butyloxycarbonyl; DiPoPE, dipalmitoleoylphosphatidylethanolamine; DMSO, dimethyl sulfoxide; DOPC, dioleoylphosphatidylcholine; DOPE, dioleoylphosphatidylethanolamine; DPX, *p*-xylene-bispyridinium bromide; DSC, differential scanning calorimetry; LUVs, large unilamellar vesicles; SUVs, small unilamellar vesicles; NBD-F, 4-fluoro-7-nitrobenz-2-oxa-1,3-diazole; *N*-NBD-PE, *N*-(7-nitrobenz-2-oxa-1,3-diazol-4-yl)phosphatidylethanolamine; *N*-Rh-PE, *N*-(lissamine rhodamine B sulfonyl)phosphatidylethanolamine; Rho, tetramethylrhodamine; PBS, phosphate-buffered saline; RP-HPLC, reverse phase high-performance liquid chromatography; T_H, bilayer to hexagonal phase transition temperature; WT, 33 N-terminal amino acids of wild-type gp41; SC, segment with the same amino acid composition as WT but with the sequence of amino acids scrambled.

Table 1: Peptide and Lipopeptide Structures

WT	AVGIGALFLGFLGAAGSTMGARS-MTLTVQARQL
(1−16)WT	AVGIGALFLGFLGAAG
(17−33)WT	STMGARSMTLTVQARQL
palmitoyl-(17−33)WT	palmitoyl-STMGARSMTLTVQARQL
palmitoyl-(17−33)SC	palmitoyl-TSMLSGRRQAMVQTTAL

In the study presented here, we investigated the relationships of rates of peptide-promoted membrane fusion to peptide length, membrane curvature, peptide structure, and arrangement in the membrane. The study utilized the 33-amino acid N-terminal peptide of gp41 of HIV as well as shorter segments of this peptide. We demonstrate different roles in membrane fusion for the segments corresponding to amino acids 1−16 and 17−33.

EXPERIMENTAL PROCEDURES

Chemicals. BOC amino acids were purchased from Novabiochem AG (Läufelfingen, Switzerland), and BOC amino acid phenylacetamidomethyl (PAM) resin was obtained from Applied Biosystems (Foster City, CA). All phospholipids were obtained from Avanti Polar Lipids (Alabaster, AL). All lipids showed one spot by TLC at a load of 50 μg. Fluorescent probes were purchased from Molecular Probes (Eugene, OR). All other chemicals and solvents were reagent grade.

Peptide Synthesis and Purification. The peptides were synthesized by a standard solid phase method on PAM-resin (0.15 mequiv) as previously described (*25*, *26*). The peptides were cleaved from the resin by HF treatment and finally precipitated with ether. All the peptides were purified by RP-HPLC on a C18 Vydac column (300 Å pore size) and were shown to be homogeneous (∼99%) by analytical HPLC. The peptide compositions were confirmed by amino acid analysis. The structures of the peptides and lipopeptides we have synthesized are summarized in Table 1.

Peptide Palmitoylation. Boc protecting groups were removed from fully protected resin-bound (17−33)WT and (17−33)SC, and palmitic acid was attached to the N-terminus as follows. Ten molar equivalents of palmitic acid dissolved in *N*,*N*-dimethylformamide and 10 molar equiv of benzotriazol-*N*-oxytris(dimethylamino)phosphonium hexafluorophosphate (BOP) were added to the resin-bound peptides suspended in 0.3 M *N*-methylmorpholine. After 2 days, uncoupled palmitic acid was removed by several washes with *N*,*N*-dimethylformamide and dichloromethane. The palmitoylated peptides were cleaved from the resin and purified as described previously.

NBD and Rho Peptide Labeling. The BOC protecting group was removed from the N-terminus of the peptides by incubation with trifluoroacetic acid (TFA), while all the other reactive amine groups of the attached peptides were kept protected. The resin-bound peptides were then treated with either (i) tetramethylrhodamine succinimidyl ester (2 equiv) in dry dimethylformamide containing 5% v/v diisopropylethylamine or (ii) NBD-F (2 equiv) in dry dimethylformamide, leading to the formation of resin-bound N^1-Rho or N^1-NBD peptides, respectively. After 72 h, the resins were washed thoroughly with DMF and then with methylene chloride. The labeled peptides were cleaved from the resin and purified as described previously.

Preparation of Large Unilamellar Vesicles (LUVs). The phospholipids and cholesterol were dissolved in a 2:1 (v/v) mixture of chloroform and methanol. The solvent was evaporated with a stream of dry nitrogen gas, depositing the lipids as a film on the walls of a Pyrex test tube. Samples were placed in a vacuum evaporator equipped with a liquid nitrogen trap for 2−3 h to remove the last traces of solvent. The dried lipid film was suspended by vigorous vortexing. The lipid suspensions were further processed with five cycles of freezing and thawing, followed by 10 passes through two stacked 0.1 mm polycarbonate filters (Nucleopore Filtration Products, Pleasanton, CA) using an Extruder (Lipex Biomembranes, Vancouver, BC) at room temperature (*27*, *28*). Lipid phosphorus was quantified by the method of Ames (*29*).

Preparation of Small Unilamellar Vesicles (SUVs). Lipid films were prepared as described above for LUVs and resuspended by vigorous vortexing. SUVs were obtained by sonication of the lipid suspensions for 2 h in a water bath-type sonicator.

Differential Scanning Calorimetry (DSC). Lipid films were made from dipalmitoleoylphosphatidylethanolamine (DiPoPE) dissolved in chloroform/methanol (2:1, v/v), and to some tubes was added a small aliquot of a solution of peptide or lipopeptide from either DMSO or trifluoroethanol. Samples of lipid alone, in the absence of peptide, were dissolved in the same organic solvent that was used for samples of that particular peptide. The organic solvent employed should have little effect on the phase behavior of the final aqueous suspension since all of the organic solvent should be eliminated during the process of making the lipid film. After solvent evaporation with nitrogen, final traces of solvent were removed in a vacuum chamber for 2 h or by overnight lyophilization when DMSO was used. The lipid films were suspended in 20 mM PIPES, 1 mM EDTA, and 150 mM NaCl with 0.002% NaN_3 (pH 7.40) by vortexing at room temperature. The final lipid concentration was 7.5 mg/mL. The lipid suspension was degassed under vacuum before being loaded into a NanoCal high-sensitivity scanning calorimeter (CSC, Provo, UT). A heating scan rate of 0.75 °C/min was generally employed. The bilayer to hexagonal phase transition was fitted using parameters to describe an equilibrium with a single van't Hoff enthalpy (*30*) and the transition temperature reported as that for the fitted curve. Data were analyzed with the program Origin, version 2.9.

Leakage Studies. Aqueous content leakage from liposomes was quantified using the ANTS-DPX assay (*31*). Films were hydrated with 12.5 mM ANTS, 45 mM DPX, 68 mM NaCl, 5 mM HEPES, 5 mM MES, and 5 mM sodium citrate (pH 7.0). The osmolarity of this solution was adjusted to be equal to that of the buffer. After being passed through a 2.5 cm × 20 cm column of Sephadex G-75, the void volume fractions were collected and the phospholipid concentration was determined by phosphate analysis. LUVs were kept in ice and used within a few hours of preparation. The fluorescence measurements were performed in 2 mL of buffer containing 5 mM HEPES, 5 mM MES, 5 mM sodium citrate, 0.15 M NaCl, and 1.0 mM EDTA (pH 7.0), in a quartz cuvette equilibrated at 37 °C. Aliquots of LUVs were added to the cuvette, and the fluorescence was recorded as a function of time using an excitation wavelength of 360 nm and an emission wavelength of 530 nm. A 490 nm cutoff filter was placed between the cuvette and the emission monochromator, and slits were set for a bandwidth of 4 nm. Leakage was started by addition of one of the peptides in a solution of DMSO. The value for 100% leakage was obtained by adding 20 μL of a 10% Triton X-100 solution to the cuvette. Controls with only the DMSO vehicle were run in all cases. All measurements were repeated at least twice, and they were in close agreement.

Lipid Mixing Assay for Membrane Fusion. The resonance energy transfer assay of Struck et al. (*32*) was used to monitor membrane fusion. Two populations of LUVs were prepared, containing DOPC, DOPE, and cholesterol at a molar ratio of 1:1:1. One portion was unlabeled and one labeled with 2 mol % *N*-Rh-PE and *N*-NBD-PE. A 9:1 molar ratio of unlabeled to labeled liposomes was used in the assay. Fluorescence was recorded at excitation and emission wavelengths of 465 and 530 nm, respectively, using a 490 nm cutoff filter placed between the cuvette and the emission monochromator, with 4 nm bandwidths, on a SLM Aminco Bowman AB-2 spectrofluorimeter. Siliconized glass cuvettes were used with continuous stirring in a thermostated cuvette holder. Measurements were carried out using 2 mL of sample in a buffer containing 5 mM Hepes, 5 mM Mes, 5 mM citric acid, 0.15 M NaCl, and 1 mM EDTA (pH 7.0). The initial residual fluorescence intensity, F_o, was taken as zero. The maximum fluorescence intensity, F_{max}, was obtained by dilution of the labeled lipids with 20 μL of 10% Triton X-100. Percent lipid mixing at time t is given by $[(F_t - F_o)/(F_{max} - F_o)]100$. In a typical experiment, LUVs at a lipid concentration of 150 μM were added to 2 mL of buffer in the cuvette at 37 °C and then the peptide was injected from a solution in DMSO. Controls with only the DMSO vehicle were run in all cases. Fluorescence was recorded for several minutes, and then 20 μL of 10% Triton X-100 was added (final concentration of 0.1%). All runs were carried out in duplicate and were found to be in close agreement using vesicles within a few hours of preparation and stored on ice.

Membrane Binding Experiments. The fluorescence of NBD is sensitive to its environment (*33*). The fluorescence quantum yield is low in solution and high in the membrane-bound state. The degree of peptide association with DOPC/DOPE/cholesterol (1:1:1) SUVs was measured by adding increasing amounts of vesicles to 0.1 μM NBD-labeled peptides dissolved in PBS. These NBD-labeled peptides exhibited the same fusogenic activity as the unlabeled peptides, as determined by electron microscopy (not shown). The fluorescence intensity was measured as a function of the lipid:peptide molar ratio, with excitation set at 467 nm (4 nm slit) and emission set at 530 nm (4 nm slit). The fluorescence values were corrected by subtracting the corresponding blank (PBS with the same amount of vesicles).

ATR-FTIR Measurements. Spectra were obtained with a Bruker equinox 55 FTIR spectrometer equipped with a deuterated triglyceride sulfate (DTGS) detector and coupled with an ATR device. For each spectrum, 150 scans were collected, with a resolution of 4 cm^{-1}. Samples were prepared as previously described (*34*). Briefly, 0.86 mg of DOPC/DOPE/cholesterol (1:1:1) alone or with peptide (lipid:peptide molar ratio of 100:1) was deposited on a ZnSe horizontal ATR prism (80 mm × 7 mm). Before sample preparation, the trifluoroacetate (CF_3COO^-) counterions, which strongly associate with the peptides, were replaced with chloride ions through several washes of the peptides in 0.1 M HCl,

followed by lyophilizations. This allowed the elimination of the strong C═O stretching absorption band near 1673 cm^{-1} (*34*). Peptides were dissolved in methanol, and lipids were dissolved in a 1:2 methanol/$CHCl_3$ mixture. Lipid/peptide mixtures or lipids with the corresponding volume of methanol were spread with a Teflon bar on the ZnSe prism. The solvents were eliminated by drying under vacuum for 20 min. Spectra corresponding to the respective pure phospholipids were subtracted from those corresponding to the lipid/peptide samples to yield the difference spectra. The background for each spectrum was a clean ZnSe prism. Hydration of the sample was achieved by introduction of an excess of deuterium oxide (^2H_2O) into a chamber placed on top of the ZnSe prism in the ATR casting and incubation for 30 min prior to acquisition of spectra. Any contribution of ^2H_2O vapor to the absorbance spectra near the amide I peak region was eliminated by subtraction of the spectra of pure lipids equilibrated with ^2H_2O under the same conditions.

ATR-FTIR Data Analysis. Prior to curve fitting, a straight baseline passing through the ordinates at 1700 and 1600 cm^{-1} was subtracted. To resolve overlapping bands, the spectra were processed using PEAKFIT (Jandel Scientific, San Rafael, CA) software. We calculated second-derivative spectra to identify the positions of the component bands in the spectra. These wavenumbers were used as initial parameters for curve fitting with Gaussian component peaks. Positions, bandwidths, and amplitudes of the peaks were varied until good agreement between the calculated sum of all components and the experimental spectra was achieved ($r^2 > 0.995$), under the following constraints: (i) the resulting bands shifted by no more than 2 cm^{-1} from the initial parameters and (ii) all the peaks had reasonable half-widths ($<20-25$ cm^{-1}). The relative contents of different secondary structure elements were estimated by dividing the areas of individual peaks, assigned to particular secondary structures (*35*), by the whole area of the resulting amide I band. The experiments were repeated twice and were found to be in good agreement.

Rhodamine Fluorescence Experiments. Rhodamine fluorescence is highly sensitive to self-quenching but poorly affected by the dielectric constant of its environment. Therefore, the tendency of the peptides to oligomerize in solution and in the membrane was tested utilizing Rho-labeled peptides. Changes in the fluorescence were measured following the addition of proteinase K (60 μg/mL final concentration) to Rho-labeled peptides (0.1 μM) previously dissolved in PBS, or in a suspension of SUVs (600 μM). Note that the [lipid]:[peptide] ratio was kept high to ensure that most of the peptide was bound to vesicles. Excitation was set at 530 nm (4 nm slit), and emission at 580 nm (4 nm slit).

RESULTS AND DISCUSSION

The 16-amino acid N-terminal fusion peptide, (1−16)-WT, lowers the T_H of DiPoPE, while the longer 33-amino acid N-terminal peptide (WT) shifts the T_H to higher temperatures (Figure 1). Since the hydrophobic segment of the peptide which enters the membrane is expected to be responsible for increasing the negative intrinsic curvature, and this segment is the same in both peptides, we can speculate that the principal effects of both peptides on the curvature properties of the membrane are similar. However, the 33-amino acid N-terminal peptide, WT, raises the T_H because of the presence of the more hydrophilic segment of residues 17−33. This segment protrudes from the membrane and inhibits bilayer−bilayer contact required for the transformation of the lamellar to the hexagonal phase. The two charged Arg residues in this segment of the molecule likely play an important role in inhibiting bilayer−bilayer contact. These results illustrate that in addition to measuring shifts in T_H one also has to take into account whether a segment of the peptide is inserted into the membrane, to accurately assess how that peptide affects membrane curvature. In cases in which there is other experimental evidence indicating which residues are inserted into the membrane or in cases, such as the present one, in which there is a very markedly nonuniform distribution of hydrophobic amino acids along the peptide chain, such an assessment can be made.

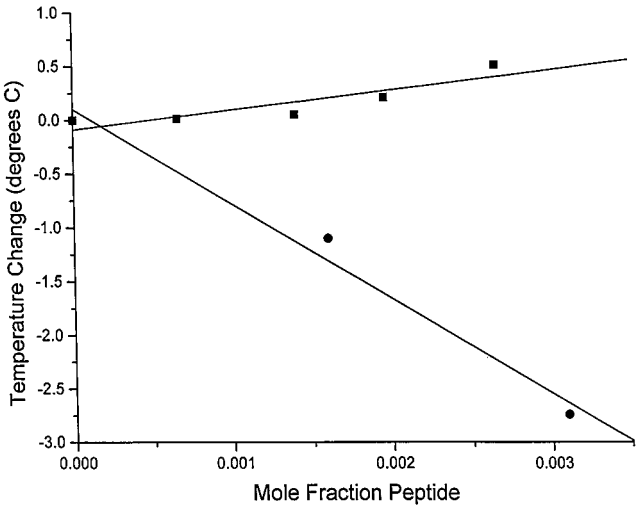

FIGURE 1: Shift of the bilayer to the hexagonal phase transition temperature of DOPE (ΔT) as a function of the mole fraction of the 16-amino acid (●) or the 33-amino acid (■) N-terminal fusion peptide of the HIV gp41. Transition temperatures were determined from DSC heating scans as described in Experimental Procedures.

We also determined how these two peptides affected the rate of lipid mixing between liposomes. It has been observed that lipid mixing using vesicles composed of DOPC, DOPE, and cholesterol is promoted by substances that increase membrane negative curvature, while it is inhibited by agents promoting positive curvature (*36*). We also find that the 16-amino acid N-terminal fusion peptide, which decreases the T_H, also promotes membrane fusion as measured by lipid mixing (Figure 2). Interestingly, however, the 33-amino acid N-terminal peptide that raises the T_H is the most potent, among the peptides studied, in promoting lipid mixing. However, if as we suggest above the curvature effects of the 16- and 33-amino acid N-terminal peptides are similar, because only the first 16 residues enter the bilayer, residues 17−33 must promote lipid mixing by a mechanism independent of membrane curvature.

We also suggest that unlike the inhibition of hexagonal phase formation by the segment of residues 17−33 of WT, this inhibition is much less important for the formation of a fusion pore. The major difference is that membrane fusion is a local event forming a single contact point between fusing bilayer membranes. In contrast, hexagonal phase formation requires the cooperative association of adjacent bilayers at

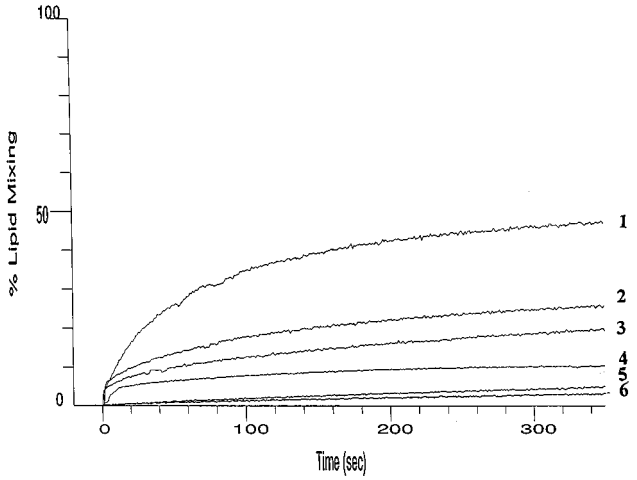

FIGURE 2: Peptide-promoted membrane fusion as determined by lipid mixing using a RET assay at 37 °C. DOPE/DOPC/cholesterol (1:1:1) LUVs at a concentration of 150 μM. Membrane fusion was promoted by 2.5 μM (1) WT, (2) palmitoyl-(17−33)WT, (3) (1−16)WT, (4) palmitoyl-(17−33)SC, (5) (17−33)WT, and (6) DMSO control.

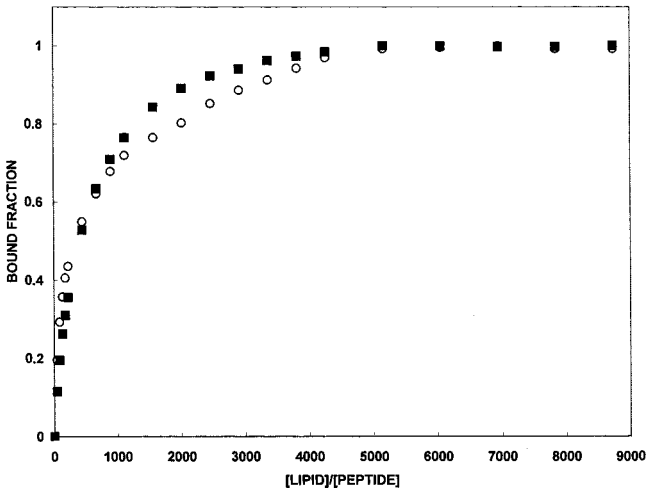

FIGURE 3: Increase in the fluorescence of NBD-labeled peptides (0.1 μM) upon titration with PC/PE/cholesterol (1:1:1) vesicles. Titrations were performed at room temperature in PBS. The excitation wavelength was set at 467 nm (4 nm slit) and emission recorded at 530 nm (4 nm slit): (○) (1−33)WT and (■) (1−16)-WT.

many points (*20*) and hence would be more readily inhibited by electrostatic repulsion between two bilayer regions containing several bound peptide chains. The pathways for formation of the hexagonal phase and the bicontinuous cubic phase (the formation of which is equivalent to the initiation of membrane fusion) are distinct (*20*). In addition, a fusion pore has been estimated from conductivity measurements to be 90 Å in diameter at its narrowest point (*37*). This is clearly sufficiently large to accommodate a short peptide fragment, and it is larger than the diameter of the aqueous core of a hexagonal phase cylinder which is around 35 Å.

The segment of amino acids 17−33 in the longer peptide is not likely to be inserted into the lipid bilayer because of its hydrophilicity. This is supported by the observation that (17−33)WT has almost no effect in promoting lipid mixing (Figure 2). However, one can facilitate the partitioning of this segment to the membrane by adding a palmitoyl group to the amino terminus. This results in the palmitoyl-(17−33)WT having lipid mixing properties comparable to those of the 16-amino acid fusion peptide (Figure 2). This is not solely a consequence of the presence of the palmitoyl moiety. Palmitic acid itself at comparable concentrations has no activity in promoting membrane fusion (not shown). An analogue of palmitoyl-(17−33)WT with the amino acid sequence of the peptide scrambled, palmitoyl-(17−33)SC, is weaker in promoting lipid mixing (Figure 2). As is suggested by the FTIR experiments (see below), it is possible that scrambling the sequence of the wild-type peptide did not completely eliminate the structures that are responsible for the lipid mixing activity. The palmitoyl-(17−33)WT is more active than (17−33)WT because of its greater extent of partitioning to a membrane. It should be noted that membrane anchoring, via a C-terminal cysteine coupled to a modified phospholipid, has been shown before to lead to fusogenic properties in a short synthetic model peptide (*38*). It is known that many membrane-disrupting lytic peptides are cationic (*39*), and this may contribute to making palmitoyl-(17−33)WT fusogenic. The WT peptide is the most active in promoting lipid mixing, and it is more active than an equimolar mixture of (1−16)WT and palmitoyl-(17−33)WT (not shown) presumably because in the WT peptide both segments can act in a cooperative fashion. An alternative explanation for the increased fusogenicity of the WT peptide, compared with that of (1−16)WT, is that it binds more strongly to the membrane. To evaluate the role of binding in the promotion of fusion, membrane binding curves of (1−33)WT and (1−16)WT were determined. The increase in the fluorescence intensity of NBD-labeled peptides due to membrane partitioning was recorded as a function of the lipid:peptide molar ratio. Binding curves are shown in Figure 3. Since rhodamine fluorescence experiments indicate that the peptides aggregate in aqueous solution (see Figure 4A), binding isotherms were not analyzed further. The shapes of the binding curves are similar, and both become saturated at about the same lipid:peptide molar ratio, suggesting that both peptides have similar affinities for DOPC/DOPE/cholesterol (1:1:1) membranes. This result indicates that the difference in the fusion activity of the peptides is not a consequence of a different binding ability, and therefore suggests a different role in fusion for the region corresponding to amino acids 17−33. If we define the fusion peptide as the segment of the fusion protein that inserts into the membrane and destabilizes a planar bilayer arrangement of the lipid, then there are additional regions of the fusion protein that also facilitate the fusion process in other ways. A similar conclusion was also drawn with regard to the influenza fusion peptide (*23*) and the Sendai virus fusion peptide (*40*).

The rapid rate of membrane fusion measured by lipid mixing with the 33-amino acid N-terminal HIV peptide is also accompanied by extensive vesicle content leakage (Figure 5). It is interesting that palmitoyl-(17−33)SC, which promotes less lipid mixing than palmitoyl-(17−33)WT, is equally potent in promoting leakage. This suggests that palmitoyl-(17−33)SC may perturb the membrane bilayer somewhat differently compared to the more fusogenic lipopeptide, palmitoyl-(17−33)WT.

Dissection of the 33-amino acid peptide into its N- and C-terminal fragments allowed us to estimate, by FTIR spectroscopy, the secondary structure content of the different

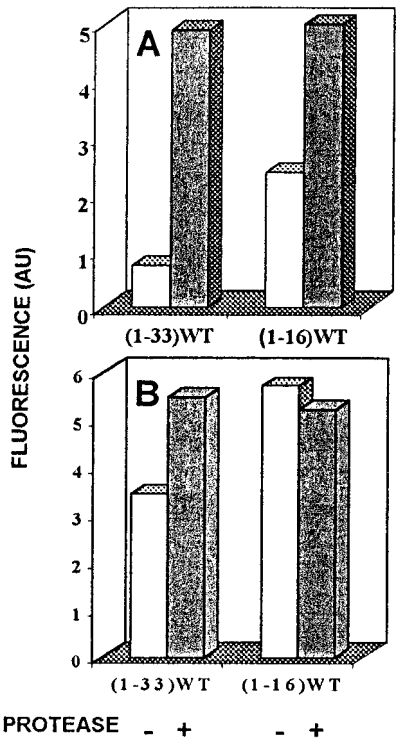

FIGURE 4: Detection of oligomerization of the peptides in aqueous solution (A) and in PC/PE/cholesterol (1:1:1) vesicles (B). (A) Rho-labeled peptides (0.1 μM) in PBS, before and 1 h after digestion with proteinase K (60 μg/mL). (B) Rho-labeled peptides (0.1 μM) bound to PC/PE/cholesterol (1:1:1) vesicles, before and 1 h after digestion with proteinase K (60 μg/mL). The excitation wavelength was set at 530 nm (4 nm slit) and the emission at 580 nm (4 nm slit).

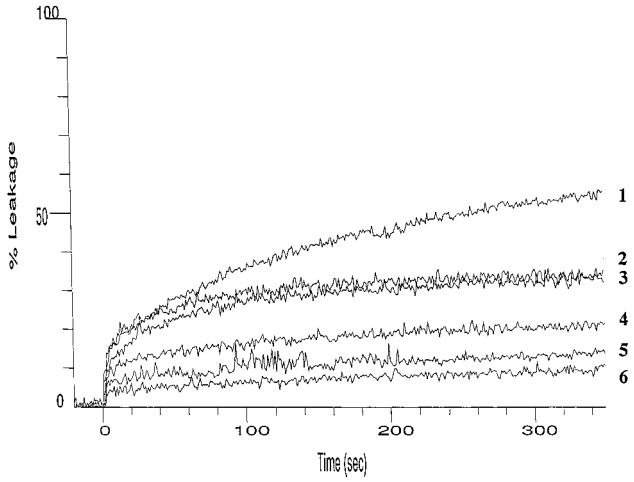

FIGURE 5: Vesicle content leakage from 75 μM DOPE/DOPC/cholesterol (1:1:1) LUVs at 37 °C with 5 μM (1) WT, (2) palmitoyl-(17−33)SC, (3) palmitoyl-(17−33)WT, (4) (1−16)WT, (5) (17−33)WT, and (6) DMSO control for spontaneous liposome leakage.

regions of the peptide when inserted into structure-promoting environments such as membranes. The spectra are shown in Figures 6 and 7, and the secondary structure content is summarized in Table 2. The 33-amino acid peptide has 50% β-sheet and 32% α-helical content, in accordance with previous observations (*7*). Furthermore, while the N-terminal fragment has 76% β-sheet content, the palmitoylated C-terminal fragment has no β-sheet structure. These results suggest that the N-terminus of the 33-amino acid peptide adopts a β-sheet secondary structure when inserted into

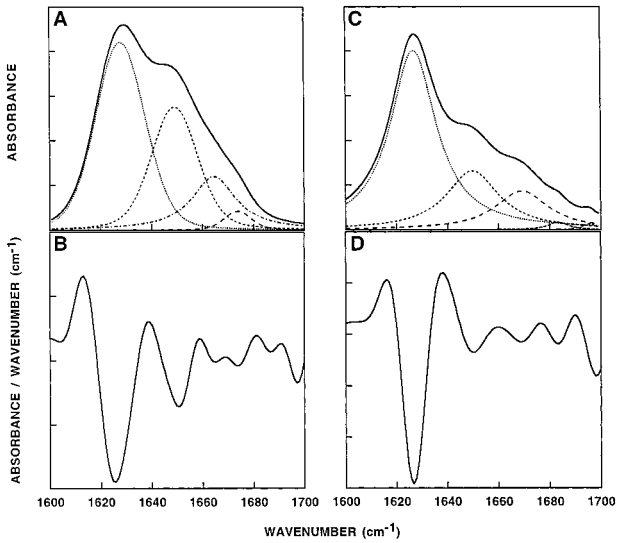

FIGURE 6: FTIR spectra deconvolution of the fully deuterated amide I band (1600−1700 cm^{-1}) of WT (A) and (1−16)WT (C) and their respective second derivatives (B and D). The component peaks are the result of curve fitting using a Voigt line shape. The amide I frequencies characteristic of the various secondary-structure elements were taken from Jackson and Mantsch (*41*). The sums of the fitted components superimpose on the experimental amide I region spectra. The solid lines represent the experimental FTIR spectra after Savitzky−Golay smoothing; the broken lines represent the fitted components of the spectra. A 100:1 lipid:peptide molar ratio was used.

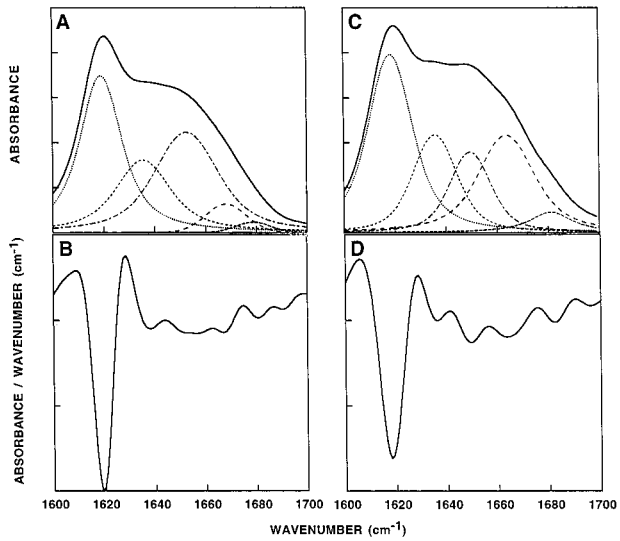

FIGURE 7: FTIR spectra deconvolution of the fully deuterated amide I band (1600−1700 cm^{-1}) of palmotoyl-(17−33)WT (A) and palmotoyl-(17−33)SC (C) and their respective second derivatives (B and D). Spectra analysis and experimental conditions were the same as those described in the legend of Figure 6.

membranes. The spectra of both palmitoyl-(17−33)WT and palmitoyl-(17−33)SC exhibited a strong peak centered around 1619 cm^{-1} that corresponds to aggregated strands (*40*), suggesting that this region could facilitate oligomerization. However, we cannot rule out the possibility that aggregation could be due to palmitoylation. While palmitoyl-(17−33)WT has 34% α-helix and 22% random coil content, the α-helical content of the scrambled peptide is only 15%. Indeed, this decrease could be related to the reduced lipid mixing ability of the scrambled peptide. From these results, a putative model can be postulated in which the first 16

Table 2: Secondary Structure Obtained for Membrane-Bound Peptides Using FTIR Spectroscopy

	secondary structure (%)[b]				
sample[a]	β-sheet	α-helix	random coil	aggregated strands	other structures
WT	50	32	−	−	18
(1−16)WT	76	23	−	−	1
palmitoyl-(17−33)WT	−	34	22	37	7
palmitoyl-(17−33)SC	−	15	20	37	28

[a] A 100:1 lipid:peptide molar ratio was used. [b] The amide I frequencies characteristic of the various secondary-structure elements were taken from Jackson and Mantsch (*40*).

amino acids of the full-length peptide are inserted into the membrane, presumably as a β-sheet, and the consecutive 17 amino acids lie near the surface of the membrane, contributing to the correct oligomerization of the peptide.

To further analyze the role of the region of residues 17−33 in the assembly of the full-length peptide in the membrane, the oligomerization state of membrane-bound (1−33)WT was compared to that of membrane-bound (1−16)WT, by self-quenching experiments with rhodamine-labeled peptides. Rhodamine fluorescence is highly sensitive to self-quenching but poorly affected by the dielectric constant of its environment. Therefore, the tendency of the peptides to oligomerize in the membrane could be tested utilizing Rho-labeled peptides. Changes in the fluorescence were measured following the addition of proteinase K to membrane-bound Rho-labeled peptides. As depicted in Figure 4B, Rho-(1−33)WT fluorescence is quenched when the peptide is bound to vesicles. Addition of proteinase K results in a disassembly of the oligomers, causing a dequenching of the Rho fluorescence. In contrast, the fluorescence of membrane-bound Rho-(1−16)WT was similar before and after the addition of the protease (actually a small decrease in the fluorescence was observed, presumably caused by the release of the Rho from the membrane), indicating that (1−16)WT does not oligomerize in the membrane. The fact that (1−16)WT was accessible to the protease was determined utilizing NBD-(1−16)WT. NBD fluorescence is sensitive to its environment, and the quantum yield is low in solution and high in the membrane-bound state. When proteinase K was added to membrane-bound NBD-(1−16)WT, a rapid decrease in the NBD fluorescence was observed (data not shown), indicating that at least part of the peptide was digested by the protease and the NBD moiety was released from the membrane. These observations suggest that the region of residues 17−33 is important for oligomerization of the full-length peptide.

In summary, our results indicate that the first 16 amino acids of the full-length peptide are inserted into the membrane, presumably as a β-sheet, and this segment promotes negative curvature which would facilitate the formation of a stalk intermediate in membrane fusion. The 17 consecutive amino acids lie near the surface of the membrane, contributing to the correct oligomerization of the peptide which further enhances its fusogenic activity.

REFERENCES

1. Chan, D. C., Fass, D., Berger, J. M., and Kim, P. S. (1997) Core structure of gp41 from the HIV envelope glycoprotein, *Cell 89*, 263−273.
2. Weissenhorn, W., Dessen, A., Harrison, S. C., Skehel, J. J., and Wiley, D. C. (1997) Atomic structure of the ectodomain from HIV-1 gp41, *Nature 387*, 426−430.
3. Rafalski, M., Lear, D., and DeGrado, W. F. (1990) Phospholipid interaction of synthetic peptides representing the N-terminus of HIV gp41, *Biochemistry 29*, 7917−7922.
4. Nieva, J. L., Nir, S., Muga, A., Goñi, F. M., and Wilschut, J. (1994) Interaction of the HIV-1 fusion peptide with phospholipid vesicles: different structural requirements for fusion and leakage, *Biochemistry 33*, 3201−3209.
5. Martin, I., Schaal, H., Scheid, A., and Ruysschaert, J.-M. (1996) Lipid membrane fusion induced by the human immunodeficiency virus type 1 gp41 N-terminal extremity is determined by its orientation in the lipid bilayer, *J. Virol. 70*, 298−304.
6. Mobley, P. W., Waring, A. J., Sherman, M. A., and Gordon, L. M. (1999) Membrane interactions of the synthetic N-terminal peptide of HIV-1 gp41 and its structural analogs, *Biochim. Biophys. Acta 1418*, 1−18.
7. Pritsker, M., Jones, P., Blumenthal, R., and Shai, Y. (1998) A synthetic all D-amino acid peptide corresponding to the N-terminal sequence of HIV-1 gp41 recognizes the wild-type fusion peptide in the membrane and inhibits HIV-1 envelope glycoprotein-mediated cell fusion, *Proc. Natl. Acad. Sci. U.S.A. 95*, 7287−7292.
8. Kliger, Y., Aharoni, A., Rapaport, D., Jones, P., Blumenthal, R., and Shai, Y. (1997) Fusion peptides derived from the HIV type 1 glycoprotein 41 associate within phospholipid membranes and inhibit cell−cell fusion. Structure−function study, *J. Biol. Chem. 272*, 13496−13505.
9. Pereira, F., Goñi, F., and Nieva, J. (1995) Liposome destabilization induced by the HIV-1 fusion peptide. Effect of a single amino acid substitution, *FEBS Lett. 362*, 243−246.
10. Brasseur, R. (1990) TAMMO: Theoretical analysis of membrane molecular organization, in *Molecular description of biological membranes by computer aided conformational analysis* (Brasseur, R., Ed.) Vol. 1, pp 203−220, CRC Press, Boca Raton, FL.
11. Brasseur, R., Vandenbranden, M., Cornet, B., Burny, A., and Ruysschaert, J.-M. (1990) Orientation into the lipid bilayer of an asymmetric amphipathic helical peptide at the N-terminus of viral fusion proteins, *Biochim. Biophys. Acta 1029*, 267−273.
12. Martin, I., Defrise-Quertain, F., Decroly, E., Vandenbranden, M., Brasseur, R., and Ruysschaert, J. M. (1993) Orientation and structure of the NH_2-terminal HIV-1 gp41 peptide in fused and aggregated liposomes, *Biochim. Biophys. Acta 1145*, 124−133.
13. Martin, I., Dubois, M. C., Defrise-Quertain, F., Saermark, T., Burny, A., Brasseur, R., and Ruysschaert, J.-M. (1994) Correlation between fusogenicity of synthetic modified peptides corresponding to the NH_2-terminal extremity of simian immunodeficiency virus gp32 and their mode of insertion into the lipid bilayer: an infrared spectroscopy study, *J. Virol. 68*, 1139−1148.
14. Horth, M., Lambrecht, B., Thiriart, C., Ruysschaert, J.-M., Burny, A., and Brasseur, R. (1991) Theoretical and functional analysis of the SIV fusion peptide, *EMBO J. 10*, 2747−2755.
15. Schaal, H., Klein, M., Gehrmann, P., Adams, O., and Scheid, A. (1995) Requirement of N-terminal amino acid residues of gp41 for human immunodeficiency virus type 1-mediated cell fusion, *J. Virol. 69*, 3308−3314.
16. Epand, R. M. (1998) Lipid polymorphism and protein-lipid interactions, *Biochim. Biophys. Acta 1376*, 353−368.
17. Colotto, A., Martin, I., Ruysschaert, J.-M., Sen, A., Hui, S. W., and Epand, R. M. (1996) Structural study of the interaction between the SIV fusion peptide and model membranes, *Biochemistry 35*, 980−989.
18. Colotto, A., and Epand, R. M. (1997) Structural study of the relationship between the rate of membrane fusion and the ability of the fusion peptide of Influenza virus to perturb bilayers, *Biochemistry 36*, 7644−7651.

19. Killian, J. A., Salemink, I., de Planque, M., Lindblom, G., Koeppe, R. E., II, and Greathouse, D. V. (1996) Induction of non-bilayer structures in diacylphosphatidylcholine model membranes by transmembrane α-helical peptides: Importance of hydrophobic mismatch and proposed role of tryptophans, *Biochemistry 35*, 1037−1045.
20. Siegel, D. P., and Epand, R. M. (1997) The mechanism of the lamellar-to-inverted hexagonal phase transitions in phosphatidylethanolamine: Implications for membrane fusion mechanisms, *Biophys. J. 73*, 3089−3111.
21. Curtain, C., Separovic, F., Nielsen, K., Craik, D., Zhong, Y., and Kirkpatrick, A. (1999) The interactions of the N-terminal fusogenic peptide of HIV-1 gp41 with neutral phospholipids, *Eur. Biophys. J. 28*, 427−436.
22. Chang, D.-K., Cheng, S.-F., and Trivedi, V. D. (1999) Biophysical characterization of the structure of the amino-terminal region of gp41 of HIV-1, *J. Biol. Chem. 274*, 5299−5309.
23. Epand, R. F., Macosko, J. C., Russell, C. J., Shin, Y.-K., and Epand, R. M. (1999) The ectodomain of HA2 of influenza virus promotes rapid pH dependent membrane fusion, *J. Mol. Biol. 286*, 489−503.
24. Slepushkin, V. A., Melikyan, G. B., Sidorova, M. S., Chumakov, V. M., Andreev, S. M., Manulyan, R. A., and Karamov, E. V. (1990) Interaction of HIV-1 fusion peptides with artificial lipid membrane, *Biochem. Biophys. Res. Commun. 172*, 952−957.
25. Merrifield, R. B., Vizioli, L. D., and Boman, H. G. (1982) Synthesis of the antibacterial peptide cecropin A (1−33), *Biochemistry 21*, 5020−5031.
26. Shai, Y., Bach, D., and Yanovsky, A. (1990) Channel formation properties of synthetic pardaxin and analogues, *J. Biol. Chem. 265*, 20202−20209.
27. Olson, F., Hunt, C. A., Szoka, F. C., Vail, W. J., and Papahadjopoulos, D. (1979) Preparation of liposomes of defined size distribution by extrusion through polycarbonate membranes, *Biochim. Biophys. Acta 557*, 9−23.
28. Mayer, L. D., Hope, M. J., and Cullis, P. R. (1986) Vesicles of variable sizes produced by a rapid extrusion procedure, *Biochim. Biophys. Acta 858*, 161−168.
29. Ames, B. N. (1966) Assay of inorganic phosphate, total phosphate and phosphatases, in *Methods in Enzymology* (Neufeld, E. F., and Ginsburg, V., Eds.) Vol. VIII, pp 115−118, Academic Press, New York.
30. Sturtevant, J. M. (1987) Biochemical applications of differential scanning calorimetry, *Annu. Rev. Phys. Chem. 38*, 463−488.
31. Ellens, H., Bentz, J., and Szoka, F. C. (1985) H^+- and Ca^{2+}-induced fusion and destabilization of liposomes, *Biochemistry 24*, 3099−3106.
32. Struck, D. K., Hoekstra, D., and Pagano, R. E. (1981) Use of resonance energy transfer to monitor membrane fusion, *Biochemistry 20*, 4093−4099.
33. Rajarathnam, K., Hochman, J., Schindler, M., and Ferguson, M. S. (1989) Synthesis, location, and lateral mobility of fluorescently labeled ubiquinone 10 in mitochondrial and artificial membranes, *Biochemistry 28*, 3168−3176.
34. Gazit, E., Miller, I. R., Biggin, P. C., Sansom, M. S. P., and Shai, Y. (1996) Structure and orientation of the mammalian antibacterial peptide cecropin P1 within phospholipid membranes, *J. Mol. Biol. 258*, 860−870.
35. Surewicz, W. K., Mantsch, H. H., and Chapman, D. (1993) Determination of protein secondary structure by Fourier transform infrared spectroscopy: a critical assessment, *Biochemistry 32*, 389−394.
36. Basañez, G., Goñi, F. M., and Alonso, A. (1998) Effect of single chain lipids on phospholipase C-promoted vesicle fusion. A test for the stalk hypothesis of membrane fusion, *Biochemistry 37*, 3901−3908.
37. Melikyan, G. B., Niles, W. D., Peeples, M. E., and Cohen, F. S. (1993) Influenza hemagglutinin-mediated fusion pores containing cells to planar membranes: flickering to final expansion, *J. Gen. Physiol. 102*, 1131−1149.
38. Pécheur, E. I., Hoekstra, D., Sainte-marie, J., Mourin, L., Bienvenüe, A., and Philippot, J. R. (1997) Membrane anchorage brings about fusogenic properties in a short synthetic peptide, *Biochemistry 36*, 3773−3781.
39. Lohner, K., and Epand, R. M. (1996) Membrane Interactions of Hemolytic and Antibacterial Peptides, *Prog. Biophys. Chem. 6*, 53−66.
40. Ghosh, J. K., and Shai, Y. (1999) Direct evidence that the N-terminal heptad repeat of Sendai virus fusion protein participates in membrane fusion, *J. Mol. Biol. 292*, 531−546.
41. Jackson, M., and Mantsch, H. H. (1995) The use and misuse of FTIR spectroscopy in the determination of protein structure, *Crit. Rev. Biochem. Mol. Biol. 30*, 95−120.

BI991887I